Proceedings of the Seventh International Conference on
Railway Technology: Research, Development and Maintenance
Edited by: J. Pombo
Civil-Comp Conferences, Volume 15, Paper 22.4
Civil-Comp Press, Edinburgh, United Kingdom, 2026
ISSN: 2753-3239, doi: 10.4203/ccc.15.22.4

Improved Railway Vibration Mitigation Through Periodic Mass-Infused Rail Pads

I. Pahari, A. Banerjee and B. Manna

Civil and Environmental Engineering, Indian Institute of Technology Delhi, New Delhi, India

Abstract

Track-induced vibrations in railway systems present persistent challenges to track durability and environmental comfort, particularly under high-speed train operations. Conventional rail pads offer limited vibration attenuation, motivating the development of improved pad configurations. The aim of this study is to propose and evaluate a periodic mass-infused rail pad (PMIRP) for enhanced vibration control in ballastless railway tracks, with its performance assessed relative to a conventional rail pad (CRP). Experimental investigations are conducted using a reduced-scale ballastless track model subjected to dynamic loading through a servo-controlled hydraulic actuator, simulating train speeds in the range of 150–300 km/h. To support the experimental observations, a mathematical dynamic model is developed to describe the vibration behaviour of the PMIRP. In addition, finite element models are established to validate the predicted dynamic responses. The embedded steel masses within the hollow cavities of the PMIRP are designed to function as local resonators, interacting with the track system to suppress vibration transmission. An H_2 optimisation approach is further employed to determine the optimal natural frequency ratio and resonator damping ratio for effective vibration reduction. The results demonstrate that the periodic mass configuration significantly enhances vibration attenuation, achieving a maximum reduction in acceleration response of up to 32.67% over the investigated speed range when compared with the CRP. The optimised PMIRP consistently outperforms the conventional design across all tested operating conditions. The findings confirm that the proposed PMIRP provides superior vibration mitigation and represents a promising solution for improving the dynamic performance of high-speed railway track systems.

Keywords: high-speed railway, experiment, under sleeper pad, optimization, railway track, ballasted track.

1 Introduction

Rail transport is widely regarded as an economical and energy-efficient solution for long-distance passenger and freight movement, effectively complementing road, air, and maritime systems. However, train operations, particularly at high speeds [1], generate significant dynamic loads [2] and high-frequency vibrations [3], which can adversely affect track infrastructure as well as the surrounding environment.

The rail pad, positioned between the rail and sleeper as an essential fastening component, plays a significant role in reducing vibrations and preserving track integrity. Its effectiveness in vibration mitigation is mainly governed by its stiffness and damping properties [4].

Widely used rail pad types in railway applications include plane rubber rail pads (PRRP), grooved rubber rail pads (GRRP), and prismatic thermoplastic polyester elastomer rail pads (PTPERP). These designs primarily reduce vibrations through adjustments in material damping and stiffness characteristics. However, achieving targeted and frequency-dependent vibration attenuation requires more advanced approaches. In this regard, the incorporation of dynamic vibration absorbers (DVAs) [5] into rail pad systems has the potential to significantly enhance performance, although such strategies remain relatively underexplored in the existing literature.

Motivated by the principle of dynamic vibration absorbers (DVAs) to enhance the vibration attenuation capability of conventional rail pads, this study introduces a novel periodic mass infused rail pad (PMIRP). The investigation is focused on improving vibration control in railway track systems using the proposed PMIRP configuration. The design incorporates steel inclusions of appropriate size, periodically embedded within the circular mesh cavities of the rail pad. These inclusions function as local resonators that respond to train-induced excitations over a range of operating speeds. During train passage, the rail undergoes vibration at the excitation frequency, which induces out-of-phase motion of the embedded resonators relative to the primary system. This mechanism facilitates energy dissipation and vibration reduction. The study further develops the mathematical formulation of both the PMIRP and conventional rail pad (CRP) systems. In addition, scaled laboratory experiments are conducted at various train speeds to evaluate and compare the vibration mitigation performance of the PMIRP against that of the CRP.

2 Geometry of Periodic Mass Infused Rail Pads (PMIRP)

Figure 1 presents periodic mass infused rail pads (PMIRP) that provide better vibration mitigation for railway tracks compared to conventional rail pads. The design includes steel masses of suitable size and design, periodically inserted into the circular mesh cavity of the proposed PMIRP. These steel masses act as vibration absorbers, improving the rail pad's vibration mitigation performance. Figure 1(a) shows a schematic diagram of the PMIRP illustrating regular circular meshes evenly distributed in the rail pad, which are further filled by steel masses. The dimensions of the scaled PMIRP are 150 × 118 × 8 mm, and the diameters of the steel balls are 12 mm. Figure 1(b) shows the fabricated PMIRP for the experiment.

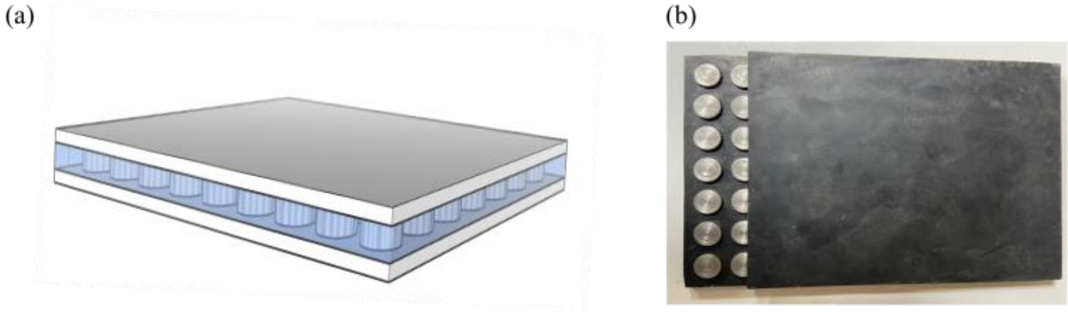

Figure 1: Configuration and physical realisation of the proposed periodic mass infused rail pad (PMIRP). (a) Schematic representation of the PMIRP; (b) fabricated PMIRP specimen prepared for experimental testing.

3 Mathematical Model of Rail Track with Rail Pad

The mathematical model of the rail supported by conventional rail pads (CRP) is shown in Fig. 2(a). The rail is represented as a lumped mass m_1, while the rail pad, primarily composed of natural rubber, is modeled as a linear spring dashpot system with stiffness $k_1$and damping coefficient c_1.

Figure 2(b) illustrates the model for the proposed periodic mass-infused rail pads (PMIRP). To ensure a consistent comparison, the rail mass $m_1$is kept identical to that in the CRP model, maintaining the same loading and excitation conditions. The PMIRP consists of two components: a primary layer equivalent to the CRP (k_1, c_1), and an auxiliary resonator system comprising a secondary mass m_2, connected via an additional spring dashpot element (k_2, c_2). This representation corresponds to a unit cell periodically distributed within the rail pad. The displacements are denoted as $X_1$for CRP, and $X_2$and $X_3$for the rail and resonator masses in PMIRP, respectively.

The amplitude magnification factor for the CRP, modeled as a single degree of freedom system, is expressed as (6):

$$M_1(\omega) = \frac{1}{\sqrt{(1-\eta^2)^2 + (2\zeta_1\eta)^2}} \qquad (1)$$

where the frequency ratio and damping ratio are defined as:

$$\eta = \frac{\omega}{\sqrt{k_1/m_1}}, \zeta_1 = \frac{c_1}{2\sqrt{m_1 k_1}} \qquad (2)$$

For the PMIRP system, the amplitude magnification factor is given by:

$$M_2(\omega) = \sqrt{\frac{(\beta^2-\eta^2)^2 + (2\zeta_2\beta\eta)^2}{[\eta^4 - (1+\beta^2+\mu\beta^2+4\zeta_2\zeta_1\beta)\eta^2 + \beta^2]^2 + 4[(\zeta_2\beta+\zeta_1)\eta^3 - (\zeta_2+\mu\zeta_2\beta^2+\zeta_1\beta)\eta]^2}} \qquad (3)$$

Here, $\beta$is the natural frequency ratio, $\eta$is the frequency ratio, $\mu$is the mass ratio, and $\zeta_1, \zeta_2$are the primary and resonator damping ratios, respectively. These parameters are defined as:

$$\beta = \frac{\sqrt{k_1/m_1}}{\sqrt{k_2/m_2}}, \qquad \eta = \frac{\omega}{\sqrt{k_1/m_1}}, \mu = \frac{m_2}{m_1}, \qquad \zeta_1 = \frac{c_1}{2\sqrt{m_1 k_1}}, \qquad \zeta_2 = \frac{c_2}{2\sqrt{m_2 k_2}} \qquad (4)$$

The excitation frequency is denoted by ω, and the natural frequency of the primary system is ω_n . In this study, the non-dimensional parameters are selected as $\beta = 1.0$, $\mu = 0.01$, $\zeta_1 = 0.08$, and $\zeta_2 = 0.01$.

Figure 2(c) compares the amplitude magnification factors $M_1(\omega)$and $M_2(\omega)$for the conventional rail pad (CRP) and the proposed periodic mass infused rail pad (PMIRP), evaluated as functions of the forced frequency ratio η. The response of the CRP system is first obtained, followed by that of the PMIRP. Within the frequency ratio range $0.58 \leq \eta \leq 1.35$, the PMIRP exhibits a notably reduced amplification compared to the CRP. This reduction indicates that, for excitation frequencies corresponding to train speeds between 150 and 300 km/h, the embedded masses in the PMIRP function as dynamic resonators. These resonators oscillate out of phase with the primary system, facilitating energy dissipation and lowering the vibration amplitude. The counteracting forces generated by the resonators effectively oppose the rail motion, thereby suppressing vibration transmission. Consequently, the rail and PMIRP interaction behaves as a coupled two-degree-of-freedom system, resulting in the splitting of resonance frequencies.

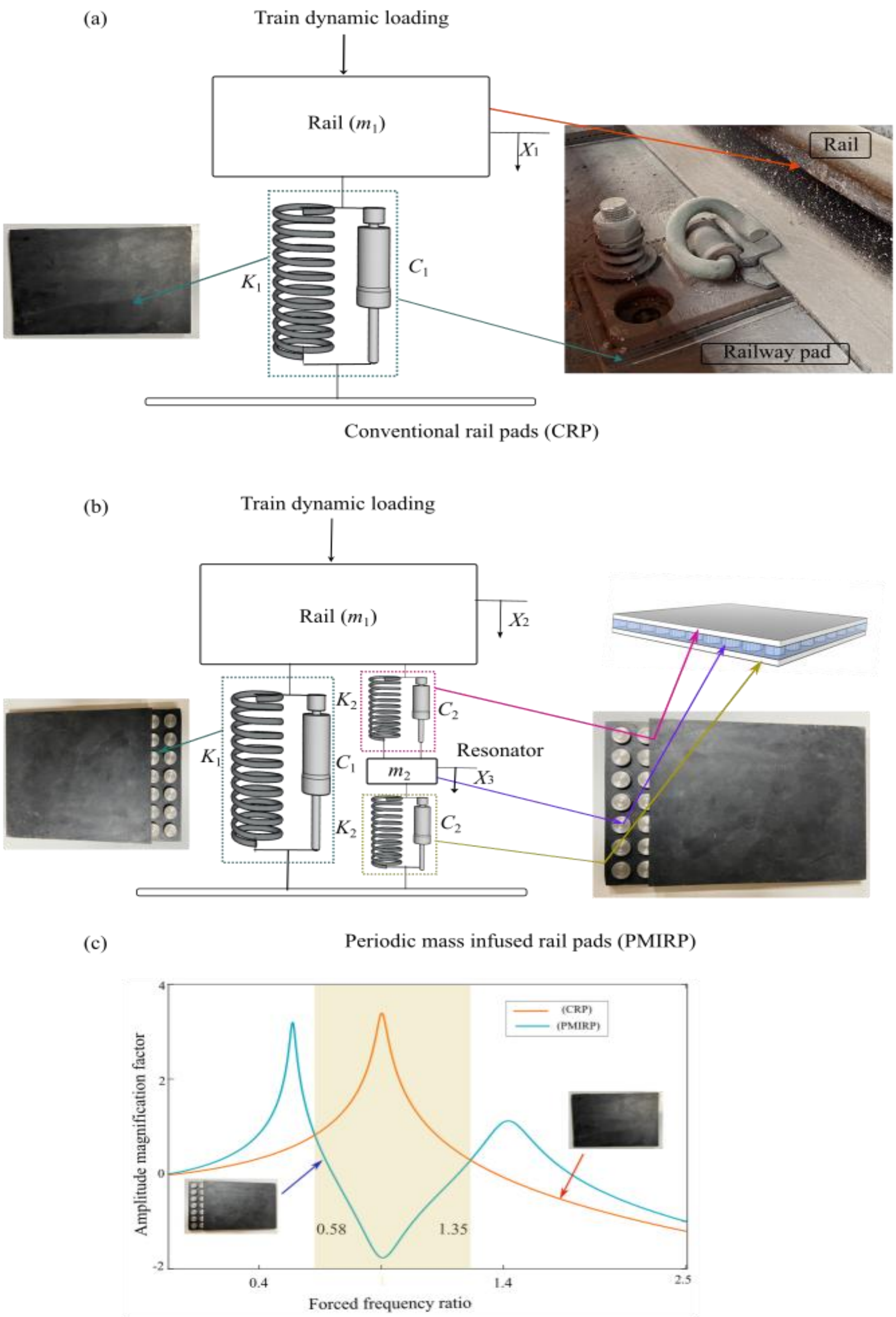

Figure 2: Mathematical representation of conventional rail pads (CRP) and periodic mass infused rail pads (PMIRP). (a) Spring–mass–dashpot model of the CRP along with its corresponding physical configuration; (b) mathematical model of the PMIRP, highlighting the spring–dashpot arrangement and the coupled spring–mass–dashpot system representing the embedded resonator; (c) frequency response of the rail mass for both CRP and PMIRP configurations.

4 Experimental Framework

This section outlines the experimental framework established to evaluate the dynamic behaviour of both conventional and proposed rail pad systems under simulated high-speed train loading. A reduced-scale railway track model is developed in a laboratory setting following Wood's 1g scaling law to ensure similarity with field conditions. The experimental arrangement comprises the track components, instrumentation, and the loading system.

4.1 Structural Representation of the Railway Track

A typical rail track system comprises a superstructure and a substructure. The superstructure includes the rail, sleeper, rail pad, concrete bearing layer (CBL), and hydraulic bounded layer (HBL), whereas the substructure consists of compacted Yamuna sand. The mechanical properties and arrangement of these layers play a critical role in governing the dynamic behaviour of both conventional rail pads and periodic mass-infused rail pads. In this study, reduced-scale laboratory experiments are conducted based on Wood's 1g scaling law [7]. A mild steel tank of dimensions 2 m × 2 m × 1.5 m is employed, as shown in Figure 3(a). The tank is initially filled with compacted Yamuna sand, over which the precast components of a ballastless track system comprising the rail, sleeper, CBL, and HBL are assembled, as shown in Figure 3(b). To ensure dynamic similitude, a scaled rail section is used in place of a full-scale UIC 60 rail. The model is developed using a scale factor of N = 2 in accordance with Wood's 1g scaling law, preserving geometric proportions while enabling accurate representation of the dynamic response under scaled loading conditions. The scaled rail thus serves as a dynamically equivalent model of the prototype. The remaining track components are fabricated following the same scaling principles. During assembly, conventional rail pads are first installed between the rail and sleeper, followed by the placement of periodic mass-infused rail pads, as illustrated in Figure 3(c). Accelerometers are mounted on different components to capture the dynamic response. The complete experimental setup, including the data acquisition system and Catman software, is shown in Figure 3(d). All experiments are conducted in the Foundation Engineering Laboratory of the Department of Civil and Environmental Engineering at the Indian Institute of Technology Delhi.

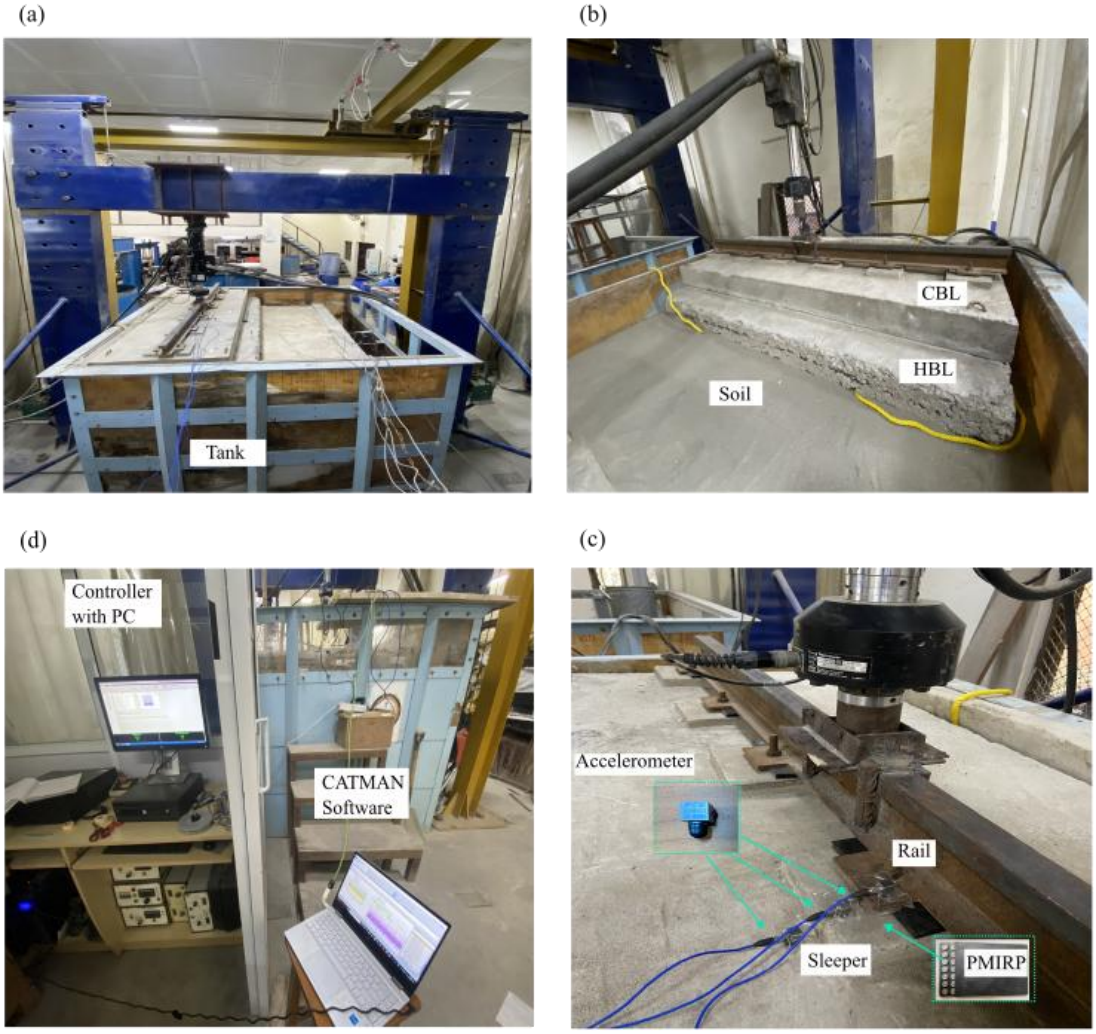

Figure 3: Scaled railway track model employed for evaluating the dynamic response of CRP and PMIRP systems. (a) Steel test tank prepared for soil backfilling; (b) assembled reduced-scale track model comprising rail, sleeper, concrete bearing layer (CBL), and hydraulic bounded layer (HBL) over compacted Yamuna sand; (c) installation of PMIRP between the rail and sleeper with accelerometers mounted for response measurement; (d) complete experimental arrangement including the instrumentation setup and Catman data acquisition system.

4.2 Dynamic Loading Profile

The loading sequence and magnitude applied through the hydraulic actuator, representing the effect of moving trains, are defined based on a validated rail crosstie foundation dynamic model [8]. The loading pattern is governed by the bogie spacing and train speed, while the load magnitude corresponds to the axle load, as illustrated in Figure 4(e) [9]. In the present study, an equivalent axle load of 20 tons is applied at train speeds of 150, 200, 250, and 300 km/h, with a constant bogie spacing of 17.5 m. The variation in dynamic wheel load with respect to train speed is summarised in Table 1, where the values are scaled according to Wood's one-gravity scaling law [7]. All relevant parameters, including wheel loads, excitation frequencies, and geometric dimensions of the track model, are scaled using a factor of N = 2. For each speed condition, 1000 loading cycles are applied using conventional rail pads. The same loading protocol is subsequently repeated after replacing the conventional pads with the proposed periodic mass-infused rail pads.

Prototype static wheel load (kN)	Dynamic wheel load (kN)	Axle load (kN) Train speed 150 km/h	Axle load (kN) Train speed 200 km/h	Axle load (kN) Train speed 250 km/h	Axle load (kN) Train speed 300 km/h
200/2	100 × (1 + 0.003V)	18.125	20.00	21.875	23.75

Table 1: Reduced scaled magnitude of wheel loading.

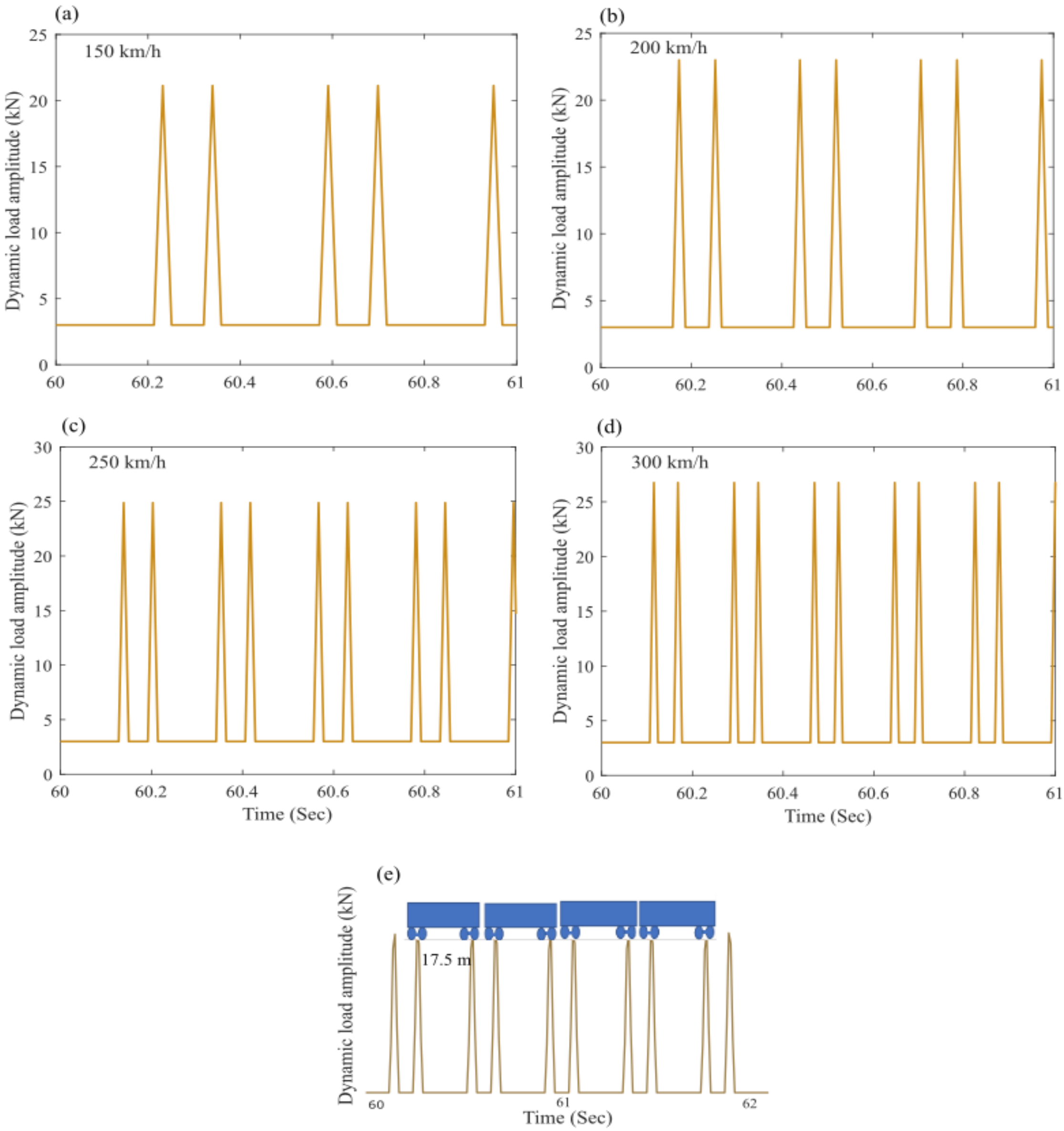

Figure 4: Dynamic loading patterns applied to the track system at different train speeds and under a representative design scenario. Subfigures (a)–(d) present the loading profiles corresponding to train speeds of 150, 200, 250, and 300 km/h, respectively. Subfigure (e) illustrates the representative loading condition developed to replicate the load distribution of a moving train, including the effect of bogie spacing.

5 Results and Discussion

Dynamic loads corresponding to train speeds of 150, 200, 250, and 300 km/h are applied using an actuator, and the resulting time-domain acceleration responses of the rail track components are recorded. Initially, conventional rail pads (CRP) are installed between the rail and sleeper, followed by the introduction of periodic mass infused rail pads (PMIRP) for comparative evaluation, as shown in Figure 5(a).

At 150 km/h, representative time–acceleration responses of the rail, sleeper, and concrete bearing layer (CBL) for both configurations are presented in Figure 5(b)–(d). The results demonstrate that PMIRP consistently yields lower acceleration levels than CRP across all components. This trend persists at higher speeds (200–300 km/h), where peak accelerations under PMIRP remain significantly reduced, indicating its enhanced vibration mitigation capability.

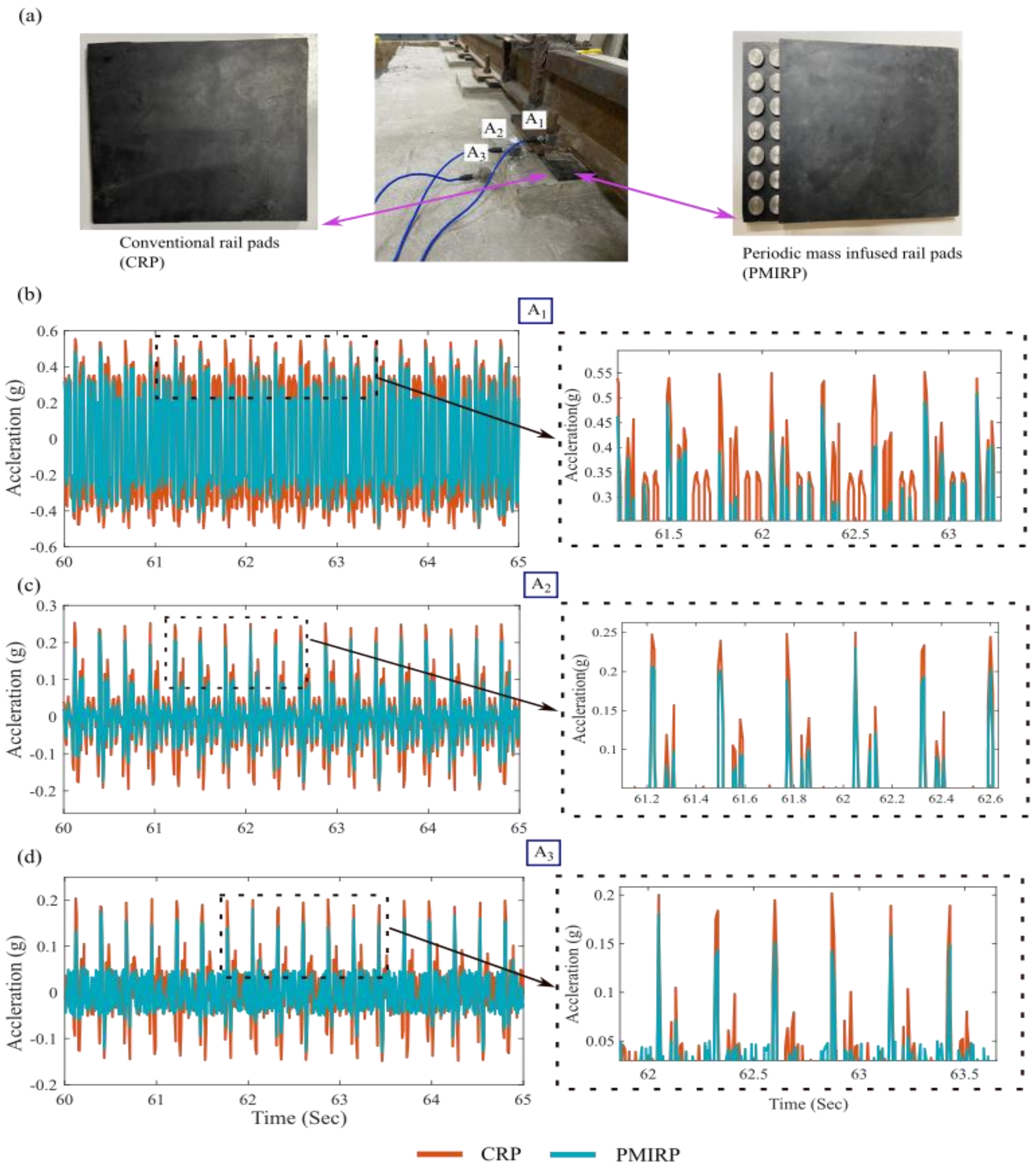

Figure 5: Time-domain comparison of vertical acceleration responses for conventional rail pads (CRP) and periodic mass infused rail pads (PMIRP) at a train speed of 150 km/h. (a) Locations of accelerometers installed on the rail, sleeper, and concrete bearing layer (CBL), identified as A1, A2, and A3; (b) vertical acceleration response of the rail with an enlarged view of peak amplitudes; (c) vertical acceleration response of the sleeper with a zoomed-in section; (d) vertical acceleration response of the CBL, including a detailed view of peak vibrations.

The observed behaviour is closely linked to the operating frequency range. When the frequency ratio η lies within 0.58–1.35, as identified earlier, the system operates within an effective attenuation zone. The tested train speeds fall within this range, resulting in reduced time-domain responses for PMIRP. This improvement is attributed to the embedded steel masses, which function as local resonators. Within the critical frequency band, these resonators oscillate out of phase with the rail, enabling energy absorption and generating counteracting forces that suppress vibration transmission. Consequently, the energy transferred to the sleeper and substructure is significantly reduced.

Figure 6 summarises the variation of maximum and average acceleration responses. A consistent reduction is observed for all components when using PMIRP. For the rail, average acceleration decreases by approximately 26.07%–32.67% over the speed range of 150–300 km/h. The sleeper exhibits a reduction of 15.27%–25.21%, while the CBL shows a decrease of 8.57%–17.47%. These results indicate that PMIRP effectively limits vibration at the source and reduces energy transmission through successive track layers.

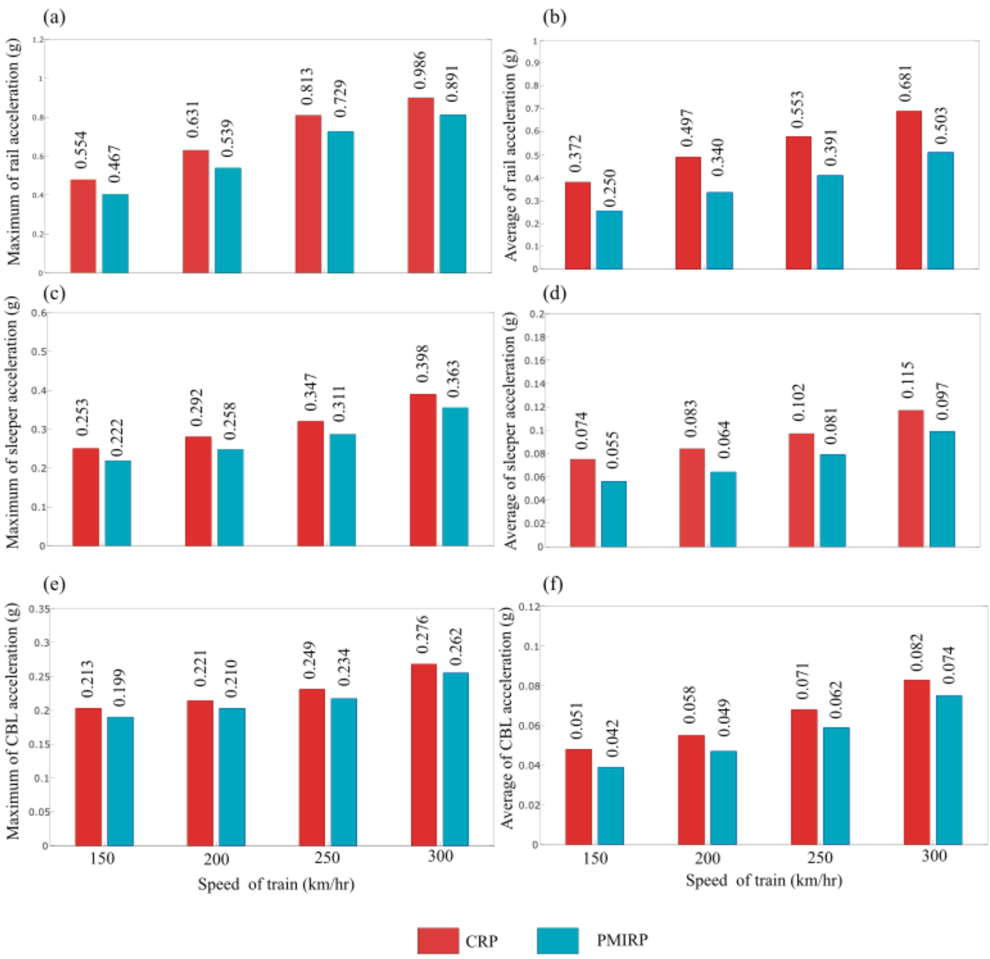

Figure 6: Comparison of maximum and average acceleration of rail, sleeper, and CBL for the CRP and PMIRP at different train speeds.

Overall, the findings demonstrate that PMIRP provides superior vibration isolation compared to conventional rail pads, making it a promising solution for high-speed railway applications.

6 Conclusions

This study presents a novel periodic mass infused rail pad (PMIRP) and evaluates its effectiveness in mitigating railway track vibrations in comparison with conventional rail pads (CRP). A reduced-scale ballastless track model incorporating PMIRP is fabricated, and dynamic responses are experimentally measured using sensors installed on track components. A key novelty lies in the design of the proposed PMIRP, where steel masses of optimised size and geometry, periodically placed within the circular mesh cavities, act as resonators that dynamically respond to train-induced vibrations across varying speeds. As the train passes, the rail vibrates at specific forcing frequencies, causing the resonators to oscillate out of phase with the primary system. This out-of-phase motion helps absorb energy and leads to a reduction in vibration amplitude. The reactive forces produced by the resonators counter the rail's vibratory motion, thereby effectively reducing track vibrations. The key findings of the study are summarised as follows:

- Experimentally, the PMIRP reduces the average rail acceleration by approximately 26.07%–32.67% for train speeds between 150 km/h and 300 km/h. Corresponding reductions in average acceleration are observed for the sleeper (15.27%–25.21%) and the concrete bearing layer (8.57%–17.47%) compared to CRP.
- The PMIRP effectively attenuates vibrations at the superstructure level, contributing to improved structural performance of the track system and reducing vibration transmission to the surrounding environment.

In summary, the proposed PMIRP demonstrates superior vibration mitigation performance relative to conventional rail pads. It offers a promising solution for railway applications, although its effectiveness can be further enhanced through appropriate tuning of design parameters for different operating speed ranges.

Acknowledgements

The authors would like to acknowledge: Scientific and Useful Profound Research Advancement, grant number SPR/2020/00278 for financial support for the project. Additionally, the authors would like to acknowledge that a patent application related to the work described in this manuscript has been filed by the Indian Institute of Technology Delhi with the Indian Patent Office.

References

[1] S. Freudenstein, *"RHEDA 2000®: Ballastless track systems for high-speed rail applications"*, International Journal of Pavement Engineering, 11 (4), 293–300, 2010.

[2] H. Gou, H. Gao, X. Ban, X. Meng, Y. Bao, *"Vibration energy transmission in high-speed railway track systems"*, Engineering Structures, 2023.

[3] S. Panda, A. Banerjee, B. Manna, *"Effectiveness of an elastically supported beam under the action of moving loads traversing in the opposite direction"*, Journal of Vibration and Control, 30 (9–10), 2093–2110, 2024.

[4] Y. Bai, Z. He, N. Bao, P. Li, *"A new mesh-type rail pad with second-order stiffness"*, Composite Structures, 232, 117763, 2024.

[5] T. Asami, O. Nishihara, A.M. Baz, *"Analytical solutions to H_∞ and H_2 optimization of dynamic vibration absorbers"*, Journal of Vibration and Acoustics, 124 (2), 284–295, 2002.

[6] J. Den Hartog, J. Ormondroyd, *"Theory of the dynamic vibration absorber"*, Transactions of the ASME, Journal of Applied Mechanics, 50 (7), 11–22, 1928.

[7] D.M. Wood, *Geotechnical Modelling*, CRC Press, 2017.

[8] H. Takemiya, X. Bian, *"Substructure simulation of inhomogeneous track and layered ground dynamic interaction under train passage"*, Journal of Engineering Mechanics, 131 (7), 2005.

[9] B. Feng, Y.I. Basarah, Q. Gu, X. Duan, X. Bian, E. Tutumluer, Y.M. Hashash, H. Huang, *"Advanced full-scale laboratory dynamic load testing of a ballasted high-speed railway track"*, Transportation Geotechnics, 29, 100559, 2021.